INVESTIGATING MASSIVE STAR FORMATION WITH THE ATACAMA LARGE MILLIMETER/SUBMILLIMETER ARRAY (ALMA) AND THE STRATOSPHERIC OBSERVATORY FOR INFRARED ASTRONOMY (SOFIA)

Zoie Telkamp[1]

Adele Plunkett[2,3] (Advisor), Rubén Fedriani[4], Jonathan Tan[1,5]

[1]Dept. of Astronomy, University of Virginia [2]National Radio Astronomy Observatory; [3]North American ALMA Science Center; [4] Instituto de Astrofísica de Andalucí, CSIC; [5]Dept. of Space, Earth & Environment, Chalmers University of Technology

Despite the huge impact that high-mass stars have on galaxy environments and the stars and planets that form within them, there is still no consensus on how they form. Leading theories include Core Accretion, i.e., a scaled-up version of low-mass star formation, and Competitive Accretion at the centers of globally collapsing protoclusters. To test these theories, we examined predictions they make on a wide range of physical scales. First, we utilized high-resolution archival ALMA data of >100 sources to investigate the inner tens- to a few hundred au where protostellar disks form. Next, we zoomed out to perform a large-scale analysis of the properties of massive protostars and their natal environments as part of the SOFIA Massive (SOMA) Star Formation Survey. This survey has observed and analyzed $>$70 massive protostars from $\sim$10-40 μm and performed global infrared spectral energy distribution fitting to estimate key properties. Together, these methods provide detailed constraints on the properties of massive protostars and the conditions required to form them.

Introduction

When studying their formation processes, stars are usually categorized as either "low mass" or "massive," where the cutoff is drawn at 8 times the mass of the sun. While the low-mass group makes up the majority of stars in the galaxy, massive stars are equally critical to the galactic environment. The radiation, winds, and supernovae produced by massive stars all output high amounts of energy that affect processes spanning the development of star clusters and planets, to the reionization of the universe. Despite their impact, the processes through which massive stars form are still debated. This is largely due to the fact that massive "protostars," or young stars that are still forming, are typically much farther away than their low-mass counterparts and are thus more difficult to observe.

The main theories of massive star formation include Core Accretion (e.g., McLaughlin & Pudritz 1997; McKee & Tan 2003; Krumholz et al. 2009) and Competitive Accretion (e.g., Bonnell et al. 1998; Wang et al. 2010; Grudić et al. 2022). Massive stars forming under Core Accretion form through a scaled-up version of the low-mass star formation process, through the collapse of self-gravitating cores that are internally supported by magnetic fields and turbulence. This process results in a central disk and a primary bipolar outflow oriented perpendicular to it. Competitive Accretion, on the other hand, predicts that massive protostars form towards the centers of dense protoclusters, where they compete for gas with surrounding low-mass protostars. As a result of interactions with these low-mass neighbors, massive stars produced via Competitive Accretion should possess truncated disks and outflows that are not necessarily perpendicular to them.

We can test these models of massive star formation by examining predictions they make on various scales. First, we will look at the inner $\sim$10s-100s of au where disks form us-

ing high-resolution, archival data from the Atacama Large Millimeter/submillimeter Array (ALMA). Then, we will zoom out and look at large-scale properties of massive protostars and their environments by discussing the SOFIA Massive Star Formation (SOMA) Survey.

Exploring Disk Scales with ALMA

Since massive protostars are typically located on kiloparsec-scale distances, observing the inner $\sim$10s-100s of au where their disks form requires very high-resolution observations. Fortunately, the Atacama Large Millimeter/submillimeter Array (ALMA) now has the capacity to make these observations. In this study, we utilized the large volumes of data available on the ALMA Science Archive to find some of the highest-resolution observations available for massive protostars. With these data, we measured fluxes, estimated properties, and compared the results to lower-mass studies to test predictions models of massive star formation make at the disk scale.

Observations

ALMA is a ground-based radio telescope located on the Chajnantor plateau in Chile. ALMA consists of 66 antennas which function as a single telescope covering a wavelength range of 0.32-3.6 mm. The ALMA Science Archive is a public database of $>$80,000 observations spanning a wide range of astronomical objects. For this study, we searched the ALMA Science Archive for Band 6 continuum data with an angular resolution of $\lesssim$50 milliarcseconds (corresponding to spatial scales of $<$200 au) under the "High-mass star formation" keyword. To facilitate this process, we used `ALminer`, a Python tool developed to enable efficient searching and visualization of data in the ALMA archive (Ahmadi & Hacar 2023). We then downloaded all continuum images meeting these guidelines that received a "Pass" quality assurance status. We visually inspected these images and retained those that contained clearly distinguishable compact continuum sources. This led to a total of 15 images of star-forming regions, most of which contain multiple sources.

Identifying Candidate Disks

To identify sources in the continuum images, we used the `Astrodendro` Python package (Robitaille et al. 2019). We set the minimum source size to the area of the synthesized beam and chose a conservative detection threshold of $5\sigma_{noise}$ to exclude lower-mass sources. This led to an initial catalog of 134 sources. Since these observations probe scales of 10s-100s of au (where disks are found) and most of the sources display an elongated shape, we will refer to these as "candidate disks". Next, we used the `IMFIT` task of the Common Astronomy Software Applications for Radio Astronomy (CASA) (CASA Team et al. 2022) (version 6.4.1) to fit a an elliptical 2D Gaussian to each continuum source. This yielded information such as the coordinate of the peak, the integrated flux of the source, and the position angle and full width at half maximum (FWHM) of the major and minor axes. After removing "poor" fits with high residuals, the final catalog consisted of 112 sources.

Candidate Candidate Disk Properties

Following Tobin et al. (2020), we estimated the radius of each candidate disk as the 2σ point of its 2D Gaussian fit after deconvolving the image from the synthesized beam. This approximately corresponds to the point that contains 90% of the total flux density, which is how Ansdell et al. (2016) defines the disk radius. To calculate the candidate disk inclinations, we used the ratio of minor and major axes, assuming circular symmetry.

Next, we estimated the dust mass corresponding to each source's measured flux den-

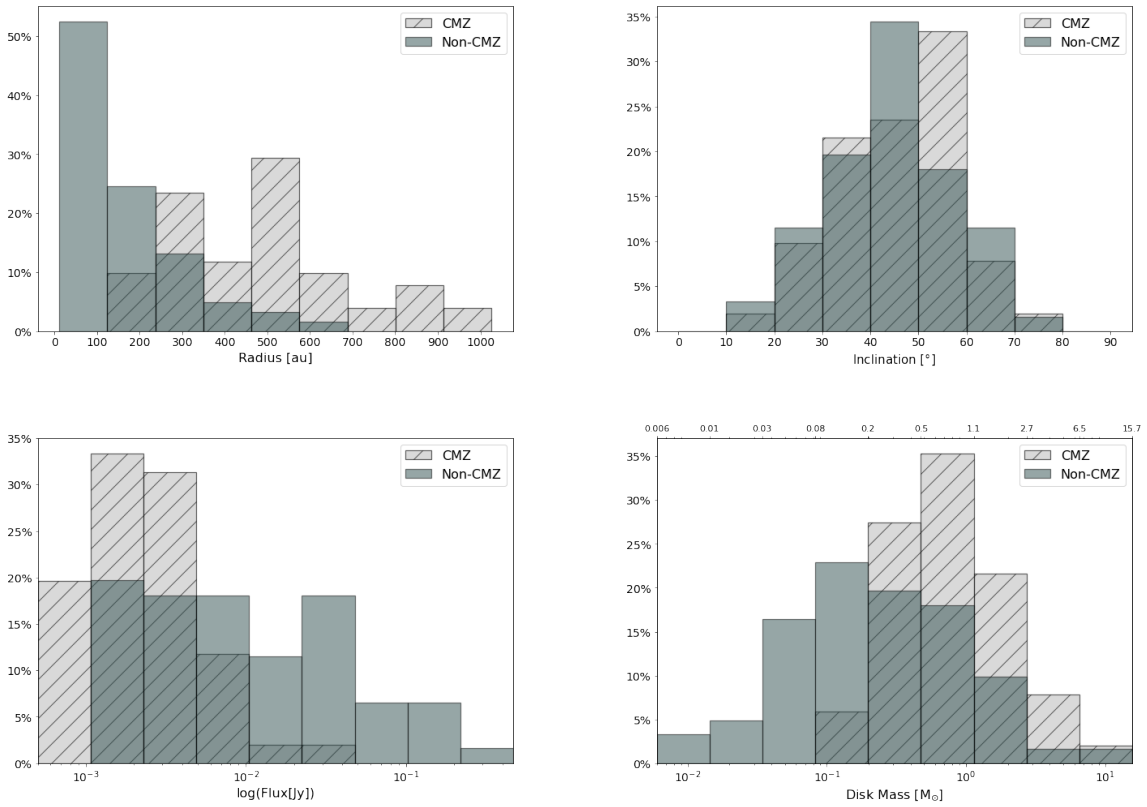

Figure 1 : Distributions of disk radius, inclination, flux, and mass calculated for sources in the CMZ (grey striped bars) and those not in the CMZ (solid bars). Note: These are preliminary results that have not yet been published.

sity (S_v) using the following equation:

$$M_{dust} = \frac{S_\nu d^2}{\kappa_\nu B_\nu(T)}, \quad (1)$$

where B_ν is the blackbody distribution flux at 1.3 mm for a dust temperature T. We calculated M_{dust} for $T = 30$ K (typical for molecular core) and then for $T = 70$ K, which is the average temperature of the envelope within $\sim 10,000$ au around a $12 - 16\ M_\odot$ protostar derived from RT simulations (see Zhang & Tan (2018)). We found the distances (d) in the literature and used an opacity of $\kappa_{1.3\text{mm}} = 0.89$ cm^2 g^{-1}, from Ossenkopf & Henning (1994). We then used a gas-to-dust ratio of 100, typical for the interstellar medium, to get the total (gas + dust) masses of the candidate disks. These values represent lower limits for the masses because Equation 1 assumes isothermal and optically thin emission, which are not necessarily true for our high-mass disk candidates.

Results and Discussion

Figure 1 shows the distributions of these calculated properties. Since half of the sources are located in the Central Molecular Zone (CMZ) — a region that is more distant than the rest of the sample and subject to more extreme conditions — we display these results separately. From the top left plot, we can see that the radii of the non-CMZ disk candidates span $\sim 10 - 600$ au, with a mean of ~ 150

au. The CMZ distribution is shifted to higher masses, spanning $\sim 150 - 1000$ au, with a mean of ~ 450 au. This could be because the CMZ is a more chaotic environment, potentially leading to larger disk radii. However, the CMZ is farther away than the rest of the sample, and the CMZ observations correspond to spatial scales of $\sim$160 au, whereas a lot of the non-CMZ observations probe spatial scales $<$100 au.

From the top right panel of Figure 1, we can see that the inclination distributions of the CMZ and non-CMZ candidate disks are similar, as we would expect. We also notice a dearth of edge-on disks (which have an inclination close to 90°) in both populations. However, this is likely due to the fact that the inclination calculations assume the disks are perfectly vertically thin, and modeling would be needed to take their actual thickness into account. From the bottom left plot of this figure, we can see that the CMZ flux values are systematically lower than the non-CMZ fluxes, likely due to the fact that the CMZ is much farther away. The bottom right panel shows that the CMZ masses are systematically higher, though this could again be due to the larger spatial scales probed by these observations.

We then compared the disk masses, inclinations, and radii of the non-CMZ sources to samples of lower-mass protostars. We tentatively found that the calculated radii were systematically larger than those of low-mass sources in Upper Sco, Orion, and Chameleon (Barenfeld et al. (2016), Tobin et al. (2020), Pascucci et al. (2016)). As such, we do not find evidence that the disks are being truncated from dynamical interactions. However, differences in the sensitivity and resolution of the datasets must be considered. It is possible that the high-mass sample observations face more contamination from inner envelope material, which would lead to larger calculated masses and radii. We are in the process of performing more robust comparisons between these samples, taking the differences in angular resolution of the observations into account.

Furthermore, the majority of the images in our sample host a primary source driving a molecular outflow. For any source that we could find CO outflow information for in the literature, we compared the position angle (PA) of this outflow to that of its disk. We approximated the disk axis orientation as the major axis PA of its 2D Gaussian fit. Figure 2 shows this comparison for three example sources. After computing the angle of separation between the outflow and disk axes, the sample displayed a tendency towards orthogonality. To assess the significance of this, we performed a Kolmogorov–Smirnov test with the null hypothesis that the deviations were randomly distributed, which yielded a p-value of 0. As such, we found tentative evidence for a preference towards perpendicular alignment for these high-mass disk candidates and their outflows, as would be expected in a Core Accretion scenario. However, the heterogeneity of the dataset and associated uncertainties must again be considered.

This project investigates high-mass star formation on scales of $\sim$10s-100s of au to test theoretical predictions of disk properies. The methods and results will be detailed in an upcoming publication (Telkamp et al., in prep). The next project I will describe zooms out to scales of $\sim$1,000 -100,000 au, where the envelope and broader star-forming core and environment are found.

The SOFIA Massive Star Formation Survey

The SOFIA Massive Star Formation (SOMA) Survey observed a large sample of intermediate- and high-mass protostars across a wide range of environments and evolutionary stages to test predictions of massive star formation theories. This sample was observed from $\sim$10 - 40 μm using the SOFIA-Faint Object infraRed CAmera for the SOFIA Telescope (FORCAST) instrument (Herter et al. 2018). The first four papers in the series (De

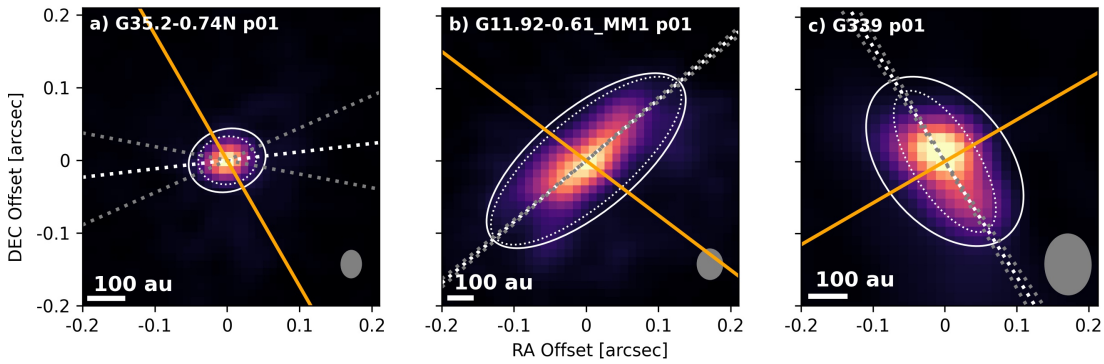

Figure 2 : 1.3 mm continuum image of three of the sources in the sample. The white ellipses represent the deconvolved 2D Gaussian fits, and the dotted gray lines show the disk axes and errors. The orange lines show the outflow axis from Sánchez-Monge et al. (2014), Cyganowski et al. (2011a), and Zhang et al. (2019). The gray ellipse in the corner of each image represents the beam area.

Buizer et al. (2017); Liu et al. (2019, 2020); Fedriani et al. (2022)) derived the properties of 40 protostars by building and fitting an infrared spectral energy distribution (SED) for each one. Fedriani et al. (2022) also presented `sedcreator`, an open-source Python package designed to facilitate the flux measurement and SED fitting process of isolated sources (https://sedcreator.readthedocs.io/). I led the SOMA V paper (Telkamp et al. 2024), where we presented 7 regions of "clustered" star formation, defined as mid-infrared sources exhibiting radio emission and surrounded by several other mid-infrared sources within ∼60". In this paper, we presented 34 total sources and looked for environmental trends in massive star formation.

Observations

The SOFIA-FORCAST observations were taken at 7.7, 19.7, 31.5, and 37.1 μm. In addition, we used archival Spitzer/IRAC (Werner et al. 2004; Fazio et al. 2004) images at 3.6, 4.5, 5.8, and 8.0 μm and Herschel/PACS and SPIRE (Griffin et al. 2010) images at 70, 160, 250, 350, and 500 μm (see SOMA I-V publications for more details on data acquisition and calibration).

Methods

To build the source SEDs, we performed aperture photometry to obtain background-subtracted flux measurements for each source. We then fit the SED of each source with the Zhang & Tan (2018) grid of radiative transfer (RT) models. We averaged the properties of the best model fits to derive key protostellar properties, such as initial core mass (M_c), mass surface density of the surrounding clump environment (Σ_{cl}), and current protostellar mass (m_*). To accomplish this, we added new and updated tools to `sedcreator`. These tools enabled us to identify sources, automate the aperture radius selection process, and build and fit SEDs in clustered regions such as these, where flux contamination from close neighbors must be accounted for. We also added a method to empirically derive the local Σ_{cl} value for a given source via graybody fitting, which can then be used to restrict the range of models considered during the SED fitting process. We discuss these updates in Telkamp et al. (2024) and will release them as `sedcreator v2.0`, which will enable efficient and uniform analysis of protostars in isolated or clustered star-forming regions.

Key Results and Discussion

After deriving protostellar properties, we investigated the environmental conditions needed to form high-mass stars. For example, a key prediction of Competitive Accretion is that high-mass star formation requires a minimum $\Sigma_{\rm cl}$ value. Below this value, the neighboring low-mass protostars would not have sufficient accretion rates and luminosities to heat up the massive core and suppress its fragmentation. Figure 3 shows the current protostellar mass (m_*) versus clump environment mass surface density ($\Sigma_{\rm cl}$) for the SOMA I-V sources, along with samples of protostars identified in infrared dark clouds (IRDCs) (Moser et al. 2020; Liu et al. 2020). The diagonal red line in this figure represents the minimum $\Sigma_{\rm cl}$ value that Krumholz & McKee (2008) predict is needed for a protostar with a given m_* to form. Under this assumption, all massive protostars should fall to the right of this line. However, the SOMA sources demonstrate a wide range of $\Sigma_{\rm cl}$ values, many of which are well below this limit. In addition, most of the $\Sigma_{\rm cl}$ values that we empirically derived through graybody fitting also lie below this threshold. Thus, these results do not provide any evidence that massive star formation requires a minimum $\Sigma_{\rm cl}$ value. Some other models of massive star formation propose alternative mechanisms for the prevention of massive core fragmentation. For example, Butler & Tan (2012) proposes that magnetic fields stronger than ~ 0.1 mG could instead be responsible for this.

Summary

We investigated massive star formation on various scales. First, we used high-resolution archival ALMA data to test predictions that Core Accretion and Competitive Accretion make on disk scales. We found that our calculated radii were systematically larger than those in several low-mass samples, in addition to noting a tentative preference towards perpendicular alignment between the disk and outflow axes. The methods and results will be detailed in an upcoming publication. Next, we utilized infrared wavelength observations of protostars in clustered regions to derive larger-scale properties of protostars and their environment as part of the SOMA Survey. These results were inconsistent with the Competitive Accretion prediction of a minimum $\Sigma_{\rm cl}$ required for high-mass stars to form. Together, these projects provide constraints on the properties of massive protostars and their disks, as well as the conditions required for their formation.

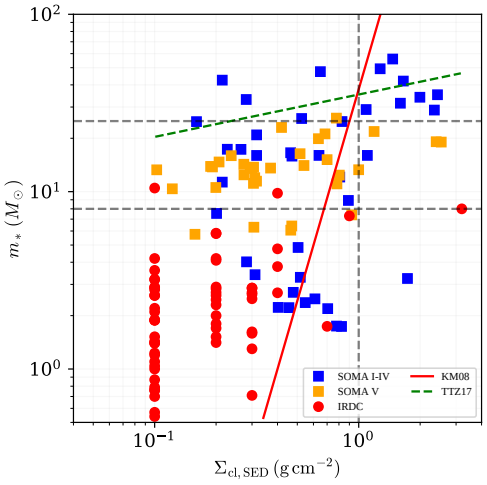

Figure 3 (Figure 12a of Telkamp et al. (2024)): Current protostellar mass (m_*) versus clump environment mass surface density ($\Sigma_{\rm cl}$) for the SOMA I-V sources and IRDC protostars. Gray dashed lines mark reference values of $m_* = 8$ and 25 $M_\odot$ and $\Sigma_{\rm cl} = 1$ g cm^{-2}. The red diagonal line shows the prediction of Krumholz & McKee (2008) (assuming their parameter values of $\delta = 1$ and $T_b = 10$ K) for the minimum $\Sigma_{\rm cl}$ needed to form a star of a given m_*.

Acknowledgments

This work is supported by the Virginia Space Grant Consortium Graduate Research STEM Fellowship Program, the National Radio Astronomy Observatory (NRAO) Summer Student Research Assistantship Program, the NRAO Graduate Student Researcher Program,

and the North American ALMA Science Center. The SOMA project briefly summarized here was carried out with the SOMA team and recieved support from the grants Juan de la Cierva, the Severo Ochoa grant, and European Union NextGenerationEU/PRTR, USRA-SOFIA, NSF, ERC, and the CCA Sabbatical Visiting Researcher program.

References

• Ahmadi et al. 2023, ALminer: ALMA archive mining and visualization toolkit, Astrophysics Source Code Library, record ascl:2306.025. • Ansdell et al. 2016, The Astrophysical Journal, 828, 46. • Barenfeld et al. 2016, ApJ, 827, 142. • Bonnell et al. 1998, MNRAS, 298, 93. • Butler et al. 2012, ApJ, 754, 5. • Cyganowski et al. 2011a, The Astrophysical Journal, 729, 124. • De Buizer et al. 2017, ApJ, 843, 33. • Fazio et al. 2004, ApJS, 154, 10. • Fedriani et al. 2022, The Astrophysical Journal, 942, 7. • Griffin et al. 2010, A&A, 518, L3. • Grudić et al. 2022, MNRAS, 512, 216. • Herter et al. 2018, Journal of Astronomical Instrumentation, 7, 1840005. • Krumholz et al. 2009, Science, 323, 754. • Krumholz et al. 2008, Nature, 451, 1082. • Liu et al. 2019, ApJ, 874, 16. • Liu et al. 2020, ApJ, 904, 75. • McKee et al. 2003, ApJ, 585, 850. • McLaughlin et al. 1997, ApJ, 476, 750. • Moser et al. 2020, ApJ, 897, 136. • Ossenkopf et al. 1994, A&A, 291, 943. • Pascucci et al. 2016, ApJ, 831, 125. • Robitaille et al. 2019, astrodendro: Astronomical data dendrogram creator, Astrophysics Source Code Library, record ascl:1907.016. • Sánchez-Monge et al. 2014, A&A, 569, A11. • Telkamp et al. 2024, The SOFIA Massive (SOMA) Star Formation Survey. V. Clustered Protostars. • Tobin et al. 2020, The Astrophysical Journal, 890, 130. • Wang et al. 2010, ApJ, 709, 27. • Werner et al. 2004, ApJS, 154, 1. • Zhang et al. 2018, ApJ, 853, 18. • Zhang et al. 2019, ApJ, 873, 73.